RSC Advances

ROYAL SOCIETY OF CHEMISTRY

www.rsc.org/advances

RSC Advances

ARTICLE

A Microfluidic Approach for the Synthesis and Assembly of Multi-Scale Porous Membranes

Received 00th January 20xx,
Accepted 00th January 20xx

DOI: 10.1039/x0xx00000x

www.rsc.org/

Minggan Li,[a] Mouhita Humanyun,[a] Bethany Hughes, [a] Janusz A Kozinski [b] and Dae Kun Hwang [a*]

A microfluidic approach is used to synthesize porous membranes with various advanced features such as multiscale pores, heterogeneous chemistry and customizable geometries. In the synthesizing process, while photomasks define microscale regular pores, polymerization-induced phase-separation forms nanoscale irregular pores. Thus, this combination offers the ability to generate multiscale pores on a membrane in a single step. The resulting membranes exhibit heterogeneous chemical properties by co-flowing prepolymer solutions with different chemical components and have designed geometries defined by photomasks. Further, complex layered structures with chemical and physical anisotropies in the cross-membrane direction can be fabricated through magnet assisted self-assembly by encapsulating magnetic particles into the membranes.

1 Introduction

Porous polymer membranes play an important role in current industry. These membranes are widely utilized in various processes such as filtration and separation,[1] water treatment,[2] protein concentration,[3] dialysis,[4] sample pre-treatment[5] and polymer electrolyte membrane (PEM) electrolysis for fuel cells.[6, 7] Two types of pore profiles are currently synthesized in polymer membranes. Irregular pores are produced via conventional membrane manufacturing methods, such as phase inversion,[8] interfacial polymerization,[9] polymer stretching[10] and electro-spinning techniques.[11] While for regular pores, lithography methods such as photolithography[12] and soft lithography[13] are utilized. These fabrication techniques have demonstrated the ability to modify mechanical and chemical properties of membranes, including tuning pore size, to meet specific requirements of industrial applications.

With the recent development of biotechnologies and microfabrication techniques, porous membranes have been increasingly explored in many lab-on-a-chip based applications, especially biochemical analysis tools and diagnostic devices. For these applications porous membranes provide core functions such as sample pretreatment and concentration,[14-18] multifraction separation,[19-21] gas sensing,[22] cell trapping and analysis,[23, 24] and bioassay.[25] Many of these applications require membranes with advanced porous features, such as multi-scale pores and heterogeneous functionality. For example, in whole-blood analysis, multi-scale pores are essential for multi-fraction separation and analysis.[26] Additionally, in chemical analysis heterogeneous functions of the membrane are needed for multiplex study.[27, 28] Despite of the critical roles of the porous membranes utilized in these applications, creating such advanced porous features is challenging. Conventional methods usually generate randomly distributed pore sizes with irregular pore profiles. These conventional methods are unable to create pores with a precise size tolerance. Although lithography methods can generate multi-scale regular pores and heterogeneous porous membranes, they are low in efficiency because of their batch process nature. Additionally, in lithography methods, creating chemically anisotropic membranes requires cumbersome multi-step alignment and protection procedures, making it a high-cost fabrication method. Despite the increasing applications for advanced porous membranes, a method to create such membranes in a cost-effective and high throughput fashion is not available.

We introduce a microfluidic synthesis route to generate porous membranes based on slit channel lithography (SCL).[29] In this route, we integrate polymerization induced phase separation (PIPS) into flow lithography, where the PIPS creates irregular nanopores while the flow lithography produces mask-defined micropores. This simple combination enables us to not only generate conventional porous membranes, but also manufacture polymeric membranes with advanced features such as multiscale pores and multifunctional membranes, in a one-step and high throughput fashion.

2 Experimental Methods

2.1 Slit channel lithography setup. The porous membrane synthesis system is based on a slit channel lithography setup.[29] In this SCL setup, a metal arc lamp was used as the UV source (Lumen 200, Prior Scientific, Rockland, MA, USA) and a UV

[a] Department of Chemical Engineering, Ryerson University, 350 Victoria Street, Toronto, Ontario, M5B 2K3, Canada
[b] Lassonde School of Engineering, York University, 4700 Keele Street, Toronto, Ontario, M3J 1P3, Canada
* Corresponding author: dkhwang@ryerson.ca
Electronic Supplementary Information (ESI) available: [details of any supplementary information available should be included here]. See DOI: 10.1039/x0xx00000x

shutter (Lambda SC, Sutter Instruments, Novato, CA, USA) was used to control the UV exposure time. A three-way solenoid valve (Model 6014, Burkert, Germany) was connected to the PDMS channel for solution feeding control. A pressure regulator (Type 100LR, ControlAir, Amherst, NH USA) was serially connected to the feeding system to adjust the feeding pressure. The UV shutter and the solenoid valve were both controlled by a program in Labview (National Instruments, Austin, TX, USA) through a digital controller (NI 9472, National Instruments, Austin, TX, USA) to coordinate the synthesis process of flow, stop, UV exposure (synthesis) and flush, in a repeating pace. An inverted microscope Axio Observer (Carl Zeiss, Jena, Germany) equipped with objectives of 5X/0.13, 10X/0.3 and 20X/0.4 (N-Achroplan, Ec plan-Neofluar and korr LD Plan-Neofluar, Carl Zeiss, Jena, Germany) was used as the synthesis platform. A UV filter set (11000v3, Chroma, VT, USA) was used to filter the UV light source to obtain desired UV excitation for polymerization. The transparency photomasks were designed with AUTOCAD 2011 and printed at a resolution of 25,000 dpi (CAD/Art Services, OR, USA).

2.2 Porous membrane synthesis. Slit PDMS channels with 60 um depth and 8 mm width were used for the membrane synthesis. The porous membranes shown in Figure 2 were synthesized using prepolymer solutions of 1% Darocur 1173 and various concentrations of Ethanol in poly(ethylene glycol) (250) diacrylate (PEG-DA 250, Sigma-Aldrich). The prepolymer solution flowing through the PDMS channel was stopped and subsequently exposed to UV light through a photomask. During UV polymerization, the applied UV light polymerized the solution into the photomask defined shapes and pores; while nanopores were obtained through polymerization induced phase separation. The synthesized porous polymer membranes were then flushed out by resuming the flow. This process can be repeated to continuously produce porous polymer membranes without sticking to the walls of the channels.

2.3 Heterogeneous porous membrane synthesis. In order to synthesize heterogeneous porous membranes, a slit PDMS channel with two inlets was used. Prepolymer solutions with 40% and 60% Ethanol respectively and 1% Darocur 1173 in PEG-DA 250 were flowed through the two inlets and three parallel streams were formed. The co-flow streams were polymerized into a heterogeneous membrane by 2 s UV light exposure through a rectangular photomask and 10 X objective.

2.4 Porous membrane assembly. To incorporate magnetic particles into membranes for magnet-assisted membrane assembly, a prepolymer solution containing 10% (v/v) magnetic beads solution (1µm, Sera-Mag, Thermo Scientific, Canada), 49% (v/v) PEG-DA 250, 40% (v/v) Ethanol and 1% (w/v) Darocur 1173 was used as the side streams and non-magnetic prepolymer solution containing 49% (v/v) PEG-DA 250, 50% (v/v) Ethanol and 1% (w/v) Darocur 1173 was used as the middle stream (Figure 4a). The co-flow streams were UV polymerized into a heterogeneous membrane by 2 s UV light exposure through a white field photomask and 10 X objective. The fabricated magnetic membranes were placed in a rectangular PDMS reservoir filled with prepolymer solution of 1% Darocur in PEG-DA 250 for assembly. As the magnetic field was applied and the solution was gently agitated by a pipette, the sheets were drawn to the corner and stacked up. When the membranes were assembled, a second UV exposure was applied through a blackfield photomask to polymerize the holes at the corners of the membranes to chemically bond them. Images were taken by charge coupled device (CCD) camera (QImaing, Canada).

2.5 SEM experiments. Samples were mounted on aluminium stubs, sputtered with 5 nm platinum and observed by a scanning electron microscopy (Quanta 3D FEG SEM, FEI Co., OR).

3 Results

3.1 Multi-scale porous membrane synthesis. Figure 1a shows the schematic of porous membrane synthesis using SCL. A UV curable prepolymer solution, containing a porogen, is flowed through a slit PDMS channel (60 µm height and 8 mm width). While the flow is stopped, a projected UV light polymerizes the prepolymer solution, facilely fabricating a polymeric membrane. During the polymerization process, oxygen diffusing via the PDMS from the surrounding inhibits the polymerization near the top and bottom PDMS walls. This oxygen inhibition layer serves as a lubrication layer at the wall [30, 31] (Figure 1b). These lubrication layers at the channel top and bottom walls ensures the synthesized membrane remains mobile, thus they can be flushed out of the channel immediately by resuming the flow. This process is repeated and membranes are fabricated continuously. The thickness and body-size of the membranes are determined by the UV dose applied and the objective magnification used at a given thickness of the PDMS channel. Furthermore, during the UV polymerization, photo lithography creates the main shape of membranes with regular micro-scale pores while PIPS forms the irregular nano-scale pores in the membranes. Therefore, this ideal combination creates multi-scale pores on geometry-customizable membranes in a single step. In addition, the co-flow properties associated to microfluidics allows the facile synthesis of heterogeneous porous membranes when different chemicals are loaded into the co-flow streams. More importantly, synthesis in microfluidic environments offers a homogenous operating condition where there is uniform distribution of UV energy across a microfluidic channel and thus uniform pore-profiles can be expected.[32, 33] Figure 1c shows a multi-scale porous membrane obtained from a UV exposure through a photo-mask. According to our previous UV polymerization studies,[29, 34] the minimum microscale pores that can be formed in our current system is about 5 µm. The enlarged image in Figure 1d displays the nanopores resulted from this process.

3.2 Controlling the morphology of the pores. By varying the process parameters, such as UV intensity, porogen concentrations and porogen types, membranes with different nanoscale morphologies can be obtained. For example, by varying the concentration of ethanol in PEG-DA from 40% to 70%, we changed the morphology of the membrane from dense to very porous structures, as shown in Figure 2. With the increase of the porogen concentration, the pore size and porosity of the membranes increase. This porous development is due to the high porogen concentration which occupies more space of the prepolymer solution and thus leave larger voids as porogen phase is separated and removed from the crosslinked polymer. As the porogen concentration increased to 80%, no polymer can be formed, because the molecular chains are separated by large amount of the porogen and their chain

growth is inhibited. At a low concentration of 40% porogen, no phase separation occurs and dense membranes are synthesized (Figure 2a). These membranes with different pore sizes and porosities show different light transparency under a phase contrast microscope, as demonstrated in Figure S1. We performed a simple mechanical property test for the membranes using a homebuilt bending tester (see Figure S2 for the details of the tests) and the results show the elastic moduli range from 1.9 MPa for 40% PEGDA and 101.2 MPa for 100% PEGDA membrane.

The morphology can also be controlled by UV intensity and porogen types. Morphological characterizations of the cross-sections of the porous membrane obtained from different UV intensities were shown in the SEM image in Figure S3. By varying the intensity of UV light changes in pore sizes and polymer globules were observed. At a high UV intensity (100% of the full intensity), the concentration of free radicals released from the photoinitiator is high and thus the photopolymerization process is fast. In a fast polymerization process, the system is unstable[35] and PIPS occurred before the gel point of the polymer, forming porous structures with connected globules, [32, 33] as shown in Figure S3d. As UV intensity decreased, the polymerization rate slowed down and the globules clump together to form larger clusters (Figure S3b). At a UV intensity of 25%, the polymer was completely cross-linked and no phase separation occurs (Figure S3a).

Different porogen types also influences the morphological properties of porous membranes. We fix the volumetric ratio of porogen to PEG-DA at 70:30 and made different porous membranes accordingly. Figure S4 shows different porogens resulting in different sized pores and polymer clusters, which are mainly determined by the difference of the solubility parameters between the porogen and the monomer. The solubility parameters of the porogens used in this study and their difference with PEG-DA are listed in Table S1. Table S1 is arranged in the increasing order of the solubility parameter difference with PEG-DA. Figure S4 shows the morphologies of membranes obtained from different porogens. As the solubility parameter difference increased, the pore size increases.

3.3 Synthesis of heterogeneous membranes. The slit channel inherits the laminar co-flow properties of microfluidics, thus, this technique allows us to make porous membranes with designed heterogeneous porosities by laterally co-flowing prepolymer solutions with various porogen concentrations in the slit channel, as schematically shown in Figure 3a. Once UV polymerized, these prepolymers solutions form into porous membranes with different morphological properties. Figure 3b, for instant, shows a membrane with three distinct porous layers: phase-separated pores in the middle (Figure 3c) and no-phase separation in the sides (Figure 3d). The microscope bright-field image in Figure 3e shows the light transmission properties of the membrane, where the porous middle part (displayed as black in Figure 3b) is opaque while the side parts are transparent. At the interface, a transitional areas present (Figure 3f) because of the diffusion of the porogen from the high to the low concentration streams during the flow and polymerization process. By controlling the diffusion process and polymerization location (upstream and downstream), we might be able to form membranes with a gradual porous profile along the lateral direction. Furthermore, various chemicals and additives can be facially loaded into co-flow streams to make membranes with chemical and functional heterogeneity if required.

3.4 Multi-layer membrane assembly. This heterogeneous fabrication ability together with the multiscale pore formation allows us to create complex layered membrane structures with advanced features. To demonstrate this fabrication ability, we create a multi-layer porous membrane with a simple lamellar structure via three steps: membrane synthesis, membrane assembly, and membrane bonding as shown in Figure 4a. In the synthesis step, we generate single membranes with three stripes - magnetic in the sides by incorporating magnetic particles and porous in the middle. Each corner of the membrane has a circular micropore for bonding purpose in the final step. In the assembly step, because the resulting porous membranes are magnetic, we can stack and align the membranes with the assistance of a magnetic field in a prepolymer-filled PDMS container. In the last step (bonding), this aligned membrane structure is chemically bonded together by projecting UV via the photomask (Figure 4a) to the corner microholes filled with the preplomer solution. Figure 4b shows the microscopy image of the resulting assembled membranes in a PDMS container and the insets are the single membranes before assembly. The assembled membrane structure has a distinctive interface because of the different pore size and porosities of the two membranes, as shown in Figure 4c. Physicochemical properties of each layer can be precisely tunable enabling us to create various lamellar porous structures with multi-layers. This assembled membrane with crosssectional morphological or chemical anisotropy may have various applications, such as 3D cell culture[36] and drug delivery[37, 38]. Providing advanced features for porous membrane structures is difficult to achieve by using conventional methods. This membrane assembly method also offers a unique layered structure fabrication route for advanced applications, such as the formation of scaffold with interconnected channel networks[39-41] and assembly of functional tissues using tissue sheets.[42, 43]

4 Conclusions

In summary, we have developed a novel method for porous membrane synthesis and assembly using slit channel lithography. We studied the effects of UV intensity, porogen concentration and porogens types on the morphological properties of membranes. By using the co-flow properties of microfluidics, we synthesized membranes with pore heterogeneity and made membranes with magnetic properties. This SCL technique not only enables us to synthesize porous membranes with multiscale pores and heterogeneities, but also allows the porous membranes to be manufactured in a one-step and high through-put fashion. With the assistance of magnetic field, we also successfully assembled membranes to form a membrane with a lamellar porous structure. This membrane synthesis technology will open up a new route for advanced porous membrane manufacturing and its application.

Acknowledgements

The authors acknowledge the Natural Sciences and Engineering Research Council of Canada (Discovery grant no. 386092 and 170464) for supporting this research.

Reference

1 L. J. Zeman and A. L. Zydney, *Microfiltration and Ultrafiltration: Principles and Applications*, CRC Press, New York, 1 edn., 1996.
2 M. A. Shannon, P. W. Bohn, M. Elimelech, J. G. Georgiadis, B. J. Marinas and A. M. Mayes, *Nature*, 2008, **452**, 301-310.
3 X. F. Zeng and E. Ruckenstein, *Journal of Membrane Science*, 1998, **148**, 195-205.
4 K. Sakai, *Journal of Membrane Science*, 1994, **96**, 91-130.
5 J. A. Jonsson and L. Mathiasson, *Journal of Chromatography A*, 2000, **902**, 205-225.
6 A. Subramania, N. T. K. Sundaram, A. R. S. Priya and G. V. Kumar, *Journal of Membrane Science*, 2007, **294**, 8-15.
7 M. Eikerling, A. A. Kornyshev, A. M. Kuznetsov, J. Ulstrup and S. Walbran, *Journal of Physical Chemistry B*, 2001, **105**, 3646-3662.
8 C. A. Smolders, A. J. Reuvers, R. M. Boom and I. M. Wienk, *Journal of Membrane Science*, 1992, **73**, 259-275.
9 Y. J. Song, P. Sun, L. L. Henry and B. H. Sun, *Journal of Membrane Science*, 2005, **251**, 67-79.
10 S. H. Tabatabaei, P. J. Carreau and A. Ajji, *Journal of Membrane Science*, 2008, **325**, 772-782.
11 P. Gibson, H. Schreuder-Gibson and D. Rivin, *Colloids and Surfaces a-Physicochemical and Engineering Aspects*, 2001, **187**, 469-481.
12 A. Revzin, R. J. Russell, V. K. Yadavalli, W. G. Koh, C. Deister, D. D. Hile, M. B. Mellott and M. V. Pishko, *Langmuir*, 2001, **17**, 5440-5447.
13 Y. N. Xia and G. M. Whitesides, *Annual Review of Materials Science*, 1998, **28**, 153-184.
14 R. S. Foote, J. Khandurina, S. C. Jacobson and J. M. Ramsey, *Analytical Chemistry*, 2005, **77**, 57-63.
15 S. Song, A. K. Singh and B. J. Kirby, *Analytical Chemistry*, 2004, **76**, 4589-4592.
16 J. Gao, J. D. Xu, L. E. Locascio and C. S. Lee, *Analytical Chemistry*, 2001, **73**, 2648-2655.
17 J. Khandurina, S. C. Jacobson, L. C. Waters, R. S. Foote and J. M. Ramsey, *Analytical Chemistry*, 1999, **71**, 1815-1819.
18 J. Lichtenberg, N. F. de Rooij and E. Verpoorte, *Talanta*, 2002, **56**, 233-266.
19 US 5096809 A, 1992.
20 H. Wei, in *Studying Cell Matabolism and Cell Interactions Using Microfluidic Devices Coupled with Mass Spectrometry*, Springer Berlin, Heidelberg, 2013, pp. 61-82.
21 H. B. Wei, B. H. Chueh, H. L. Wu, E. W. Hall, C. W. Li, R. Schirhagl, J. M. Lin and R. N. Zare, *Lab on a Chip*, 2011, **11**, 238-245.
22 S. M. Mitrovski, L. C. C. Elliott and R. G. Nuzzo, *Langmuir*, 2004, **20**, 6974-6976.
23 J. R. Rettig and A. Folch, *Analytical Chemistry*, 2005, **77**, 5628-5634.
24 S. Yamamura, H. Kishi, Y. Tokimitsu, S. Kondo, R. Honda, S. R. Rao, M. Omori, E. Tamiya and A. Muraguchi, *Analytical Chemistry*, 2005, **77**, 8050-8056.
25 P. Kim, H. E. Jeong, A. Khademhosseini and K. Y. Suh, *Lab on a Chip*, 2006, **6**, 1432-1437.
26 J. Moorthy and D. J. Beebe, *Lab on a Chip*, 2003, **3**, 62-66.
27 P. J. Bracher, M. Gupta and G. M. Whitesides, *Soft Matter*, 2010, **6**, 4303-4309.
28 P. J. Bracher, M. Gupta, E. T. Mack and G. M. Whitesides, *Acs Applied Materials & Interfaces*, 2009, **1**, 1807-1812.
29 M. G. Li, M. Humayun, J. A. Kozinski and D. K. Hwang, *Langmuir*, 2014, **30**, 8637-8644.
30 D. Dendukuri, S. S. Gu, D. C. Pregibon, T. A. Hatton and P. S. Doyle, *Lab on a Chip*, 2007, **7**, 818-828.
31 D. Dendukuri, P. Panda, R. Haghgooie, J. M. Kim, T. A. Hatton and P. S. Doyle, *Macromolecules*, 2008, **41**, 8547-8556.
32 S. Dubinsky, H. Zhang, Z. H. Nie, I. Gourevich, D. Voicu, M. Deetz and E. Kumacheva, *Macromolecules*, 2008, **41**, 3555-3561.
33 S. Dubinsky, J. Il Park, I. Gourevich, C. Chan, M. Deetz and E. Kumacheva, *Macromolecules*, 2009, **42**, 1990-1994.
34 M. G. Li, N. Hakimi, R. Perez, S. Waldman, J. A. Kozinski and D. K. Hwang, *Advanced Materials*, 2015, **27**, 1880-+.
35 K. F. Luo, *European Polymer Journal*, 2006, **42**, 1499-1505.
36 Y. Wang, A. A. Ahmad, P. K. Shah, C. E. Sims, S. T. Magness and N. L. Allbritton, *Lab on a Chip*, 2013, **13**, 4625-4634.
37 R. Neubert, C. Bendas, W. Wohlrab, B. Gienau and W. Furst, *International Journal of Pharmaceutics*, 1991, **75**, 89-94.
38 R. Neubert, W. Wohlrab and C. Bendas, *Prediction of Percutaneous Penetration*, 1990, 431-436.
39 A. P. Golden and J. Tien, *Lab on a Chip*, 2007, **7**, 720-725.
40 B. J. Papenburg, J. Liu, G. A. Higuera, A. M. C. Barradas, J. de Boer, C. A. van Blitterswijk, M. Wessling and D. Stamatialis, *Biomaterials*, 2009, **30**, 6228-6239.
41 W. Lee, V. Lee, S. Polio, P. Keegan, J. H. Lee, K. Fischer, J. K. Park and S. S. Yoo, *Biotechnology and Bioengineering*, 2010, **105**, 1178-1186.
42 Y. Haraguchi, T. Shimizu, T. Sasagawa, H. Sekine, K. Sakaguchi, T. Kikuchi, W. Sekine, S. Sekiya, M. Yamato,

M. Umezu and T. Okano, *Nature Protocols*, 2012, **7**, 850-858.
43 E. G. Roberts, E. L. Lee, D. Backman, J. A. Buczek-Thomas, S. Emani and J. Y. Wong, *Annals of Biomedical Engineering*, 2015, **43**, 762-773.

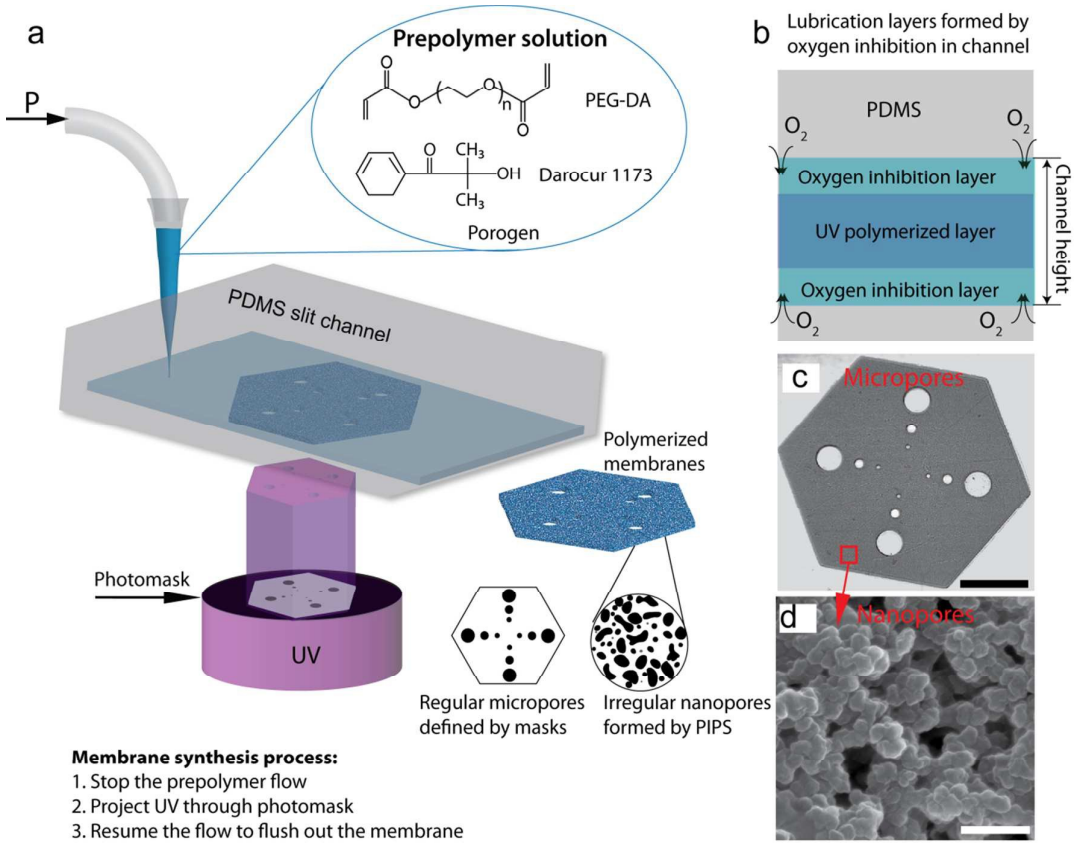

Figure 1. Porous membrane synthesis using slit channel lithography. a) Schematic of SCL. A prepolymer solution is flowed in a PDMS slit channel and is polymerized by UV light through a photomask as the flow is paused. After UV polymerizatioin, the synthesized membrane is flushed out of the channel by resuming the flow. The process is repeated and membranes can be synthesized continuously. b) Oxygen inhibition at the channel walls forms lubrication layers for membrane flush. c and d) SEM images show the micro and nano pores formed in a single step polymerization. Scale bars are 1mm (c) and 1 µm (d).

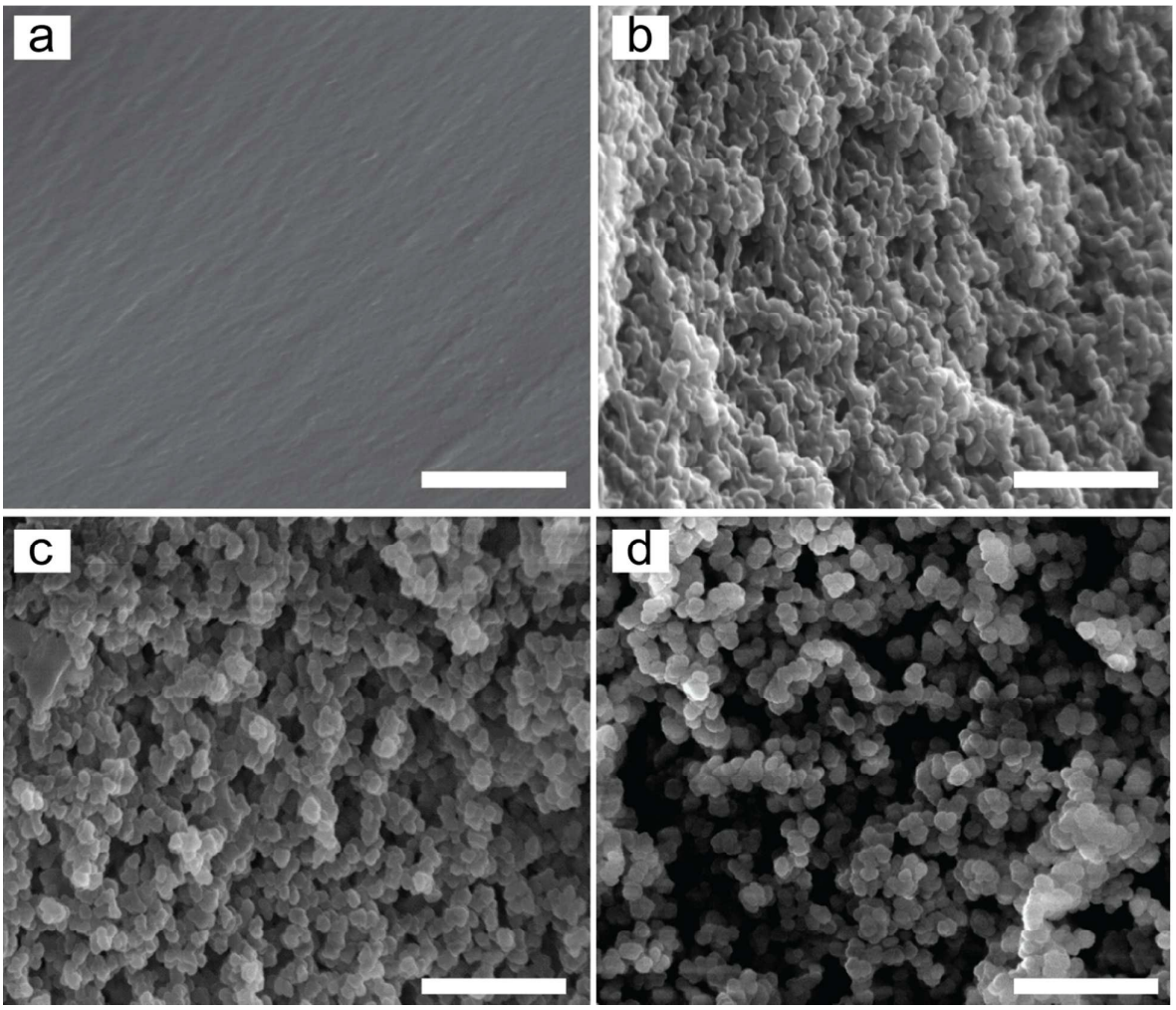

Figure 2. SEM cross sectional image of porous polymer membranes fabricated using slit channel lithography. A mixture of ethanol (porogen) and (PEG-DA 250 + 1.0% photoinitiator) at 2 seconds exposure and full UV intensity was used. a) 40% ethanol, b) 50% ethanol, c) 60% ethanol, and d) 70% ethanol. Scale bars are 2 µm.

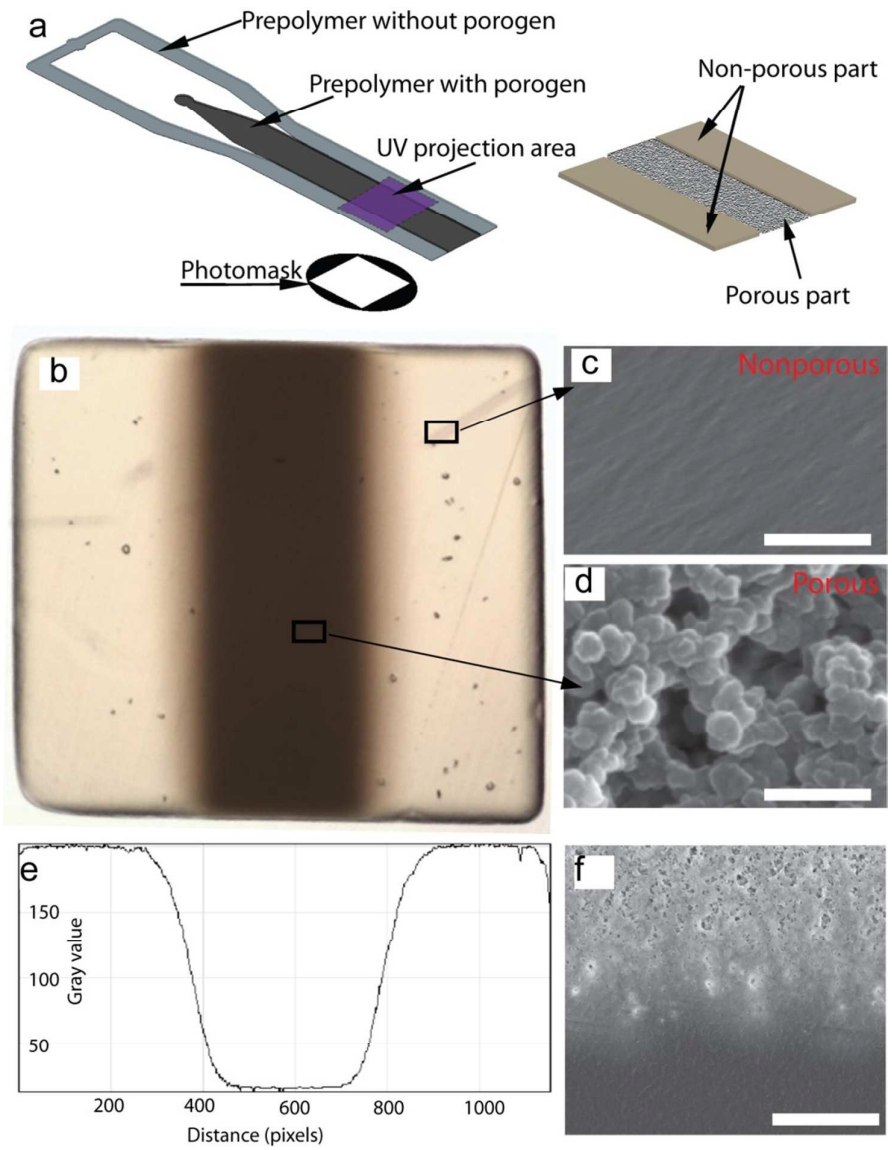

Figure 3. Heterogeneous porous polymer membranes fabricated using slit channel lithography. a) Schematic of heterogeneous membrane synthesis by using co-flow. b) Bright-field image of a square shaped heterogeneous porous polymer membrane. c) SEM images showing the dense and porous part of the membrane. e) Plot of gray-scale intensity along the surface of the membrane in b), and e) A SEM image of the interface between a side and middle part of a heterogeneous porous membrane. Scale bares are 1 µm (c and d) and 10 µm (e).

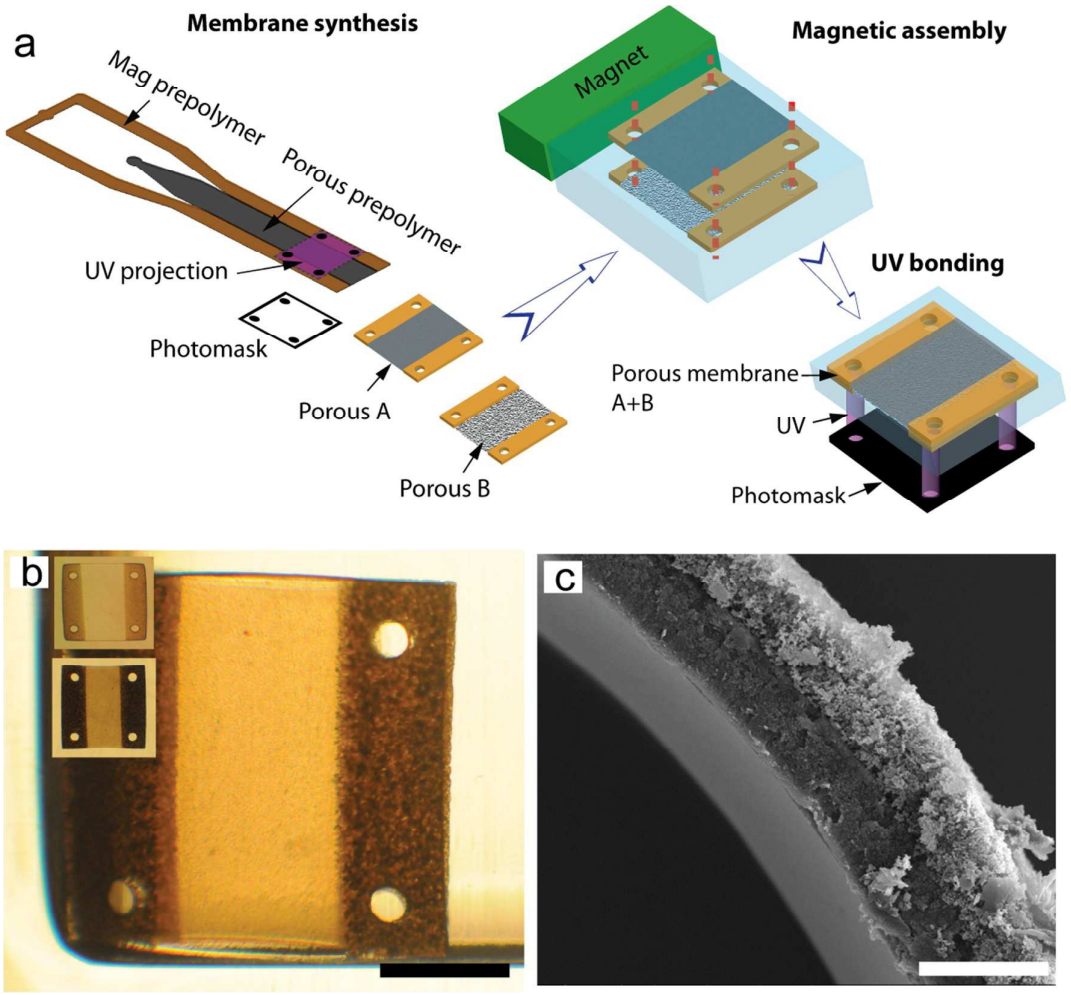

Figure 4. Multilayer membrane assembly. a) Schematic of magnetic porous membrane synthesis and assembly. In a slit channel, a PEG-DA solution with 10% magnetic suspension is used as the two side streams to generate membranes with magnetic property and PEG-DA solution is used in the middle stream to create porous part of the membrane. b) A bright-field image of an assembled membrane. Insets are the membrane before assembly. c) A SEM image showing the cross section of the assembled membranes. Scale bars are 1 mm (c) and 50 μm (d).

Entry for the Table of Contents

Polymeric porous membranes with multiscale pores and heterogeneous functions are synthesized in a one-step fashion using a microfluidic approach.